Eur Biophys J (2001) 30: 83–90
DOI 10.1007/s002490000122

ARTICLE

**Luana Scheffer · Arkady Bitler
Eshel Ben-Jacob · Rafi Korenstein**

Atomic force pulling: probing the local elasticity of the cell membrane

Received: 7 July 2000 / Revised version: 26 October 2000 / Accepted: 26 October 2000 / Published online: 6 February 2001

Abstract We present a novel approach, based on atomic force microscopy, for exploring the local elastic properties of the membrane-skeleton complex in living cells. Three major elements constitute the basis for the proposed method: (1) pulling the cell membrane by increasing the adhesion of the tip to the cell surface provided via appropriate tip modification; (2) measuring force-distance curves with emphasis on selecting the appropriate withdrawal regions for analysis; (3) fitting of the theoretical model for axisymmetric bending of an annular thick plate to the experimental curve in the withdrawal region, prior to the detachment point of the tip from the cell membrane. This approach, applied to human erythrocytes, suggests a complimentary technique to the commonly used methods. The local use of this methodology for determining the bending modulus of the cell membrane of the human erythrocyte yields a value of $(2.07 \pm 0.32) \times 10^{-19}$ J.

Keywords Erythrocyte membrane · Bending modulus · Atomic force microscopy · Tip coating · Force-distance curve

Introduction

The mechanical behavior of the complex of a cell membrane with the underlying protein network, forming the cortical skeleton, plays an essential role in vital cellular functions such as endocytosis, cell motility or cell division. Since the red blood cell (RBC) is among the simplest and best characterized cellular systems, which undergoes mechanical deformations during blood circulation, the mechanical behavior of its membrane-skeleton complex has been extensively studied. The deformability of the red blood cell has been measured using various methods, including filtration (Koutsoris et al. 1988), rheoscopy (Schmid-Schoenbein et al. 1973), ektacytometry (Groner et al. 1980), microaspiration (Evans et al. 1976) and flicker spectroscopy (Brochard and Lennon 1975). However, only the last two methods yielded a quantitative estimation of the elastic modulus of the erythrocyte's membrane-skeleton complex (Evans 1983; Zilker et al. 1992; Strey et al. 1995). From microaspiration measurements it was estimated that the upper boundary value of the bending modulus of a human erythrocyte is 1.8×10^{-19} J (Evans 1983). Previous results obtained by flicker spectroscopy yielded a range of values of $1.3–3 \times 10^{-20}$ J (Brochard and Lennon 1975). Further microinterferometry combined with fast image processing yielded a similar value of 2.3×10^{-20} J (Zilker et al. 1992). Nevertheless, recent measurements based on phase contrast microscopy combined with fast image processing suggest a significantly larger range of bending modulus values of $2–7 \times 10^{-19}$ J (Strey et al. 1995).

Atomic force microscopy (AFM) offers a complementary methodology, which enables measuring the local variation of the mechanical properties over a cell's surface. AFM, introduced in 1986 (Binnig et al. 1986), is well known for its high-resolution topographic images and high-accuracy measurements of a wide variety of sample surface characteristics on a microscopic scale. Of great importance for applications in biology is the potential use of AFM to the study of soft samples in their physiological environment (Bezanilla et al. 1994; Thomson et al. 1996). Moreover, AFM has been applied to measuring the strength of ligand-receptor interaction with the ligands attached to the measuring tip (Florin et al. 1994; Allen et al. 1997). Recently, AFM was widely used to explore the

L. Scheffer and A. Bitler contributed equally.

L. Scheffer · A. Bitler · R. Korenstein (✉)
Department of Physiology and Pharmacology,
Sackler School of Medicine,
Tel-Aviv University, Tel-Aviv 69978, Israel
E-mail: korens@post.tau.ac.il
Tel.: +972-3-6406042; Fax: +972-3-6408982

L. Scheffer · E. Ben-Jacob
Department of Condensed Matter,
School of Physics and Astronomy,
Tel-Aviv University, Tel-Aviv 69978, Israel

elastic properties of biological samples. A closer insight into the mechanical properties of cells is obtained from AFM force-distance curves, in which the tip is first lowered into contact with the sample, then indents the surface and, finally, lifts off the sample's surface. Since this technique averages properties on a nanometric scale, it was used to probe the elastic properties of various biological structures with a relatively high spatial resolution. For example, the elastic moduli were measured on platelets (Radmacher et al. 1996), glial cells (Haydon et al. 1996), atrial myocytes (Shroff et al. 1995), cholinergic synaptic vesicles (Laney et al. 1997) and MCDK cells (Hoh and Schoenenberger 1994). Nevertheless, the applied indentation technique suffers from certain difficulties in quantitatively analyzing the force-distance data. One of the most vexing problems is the accurate finding of the contact point between the tip and the sample. A small uncertainty in the determination of the tangent to the slope in the contact region leads to significant errors in the estimation of the point of contact, the indentation depth and the consequent calculation of elastic moduli based on the commonly used Hertz model (A-Hassan et al. 1998). Moreover, the indentation technique can yield a spurious stiffening effect when measuring thin biological samples, owing to the interference of the substrate.

The present study suggests a complementary method for the measurement of the elastic properties of living cells, which encompasses the advantages of both the microaspiration technique and the AFM-based indentation method. At the same time, it resolves the problems related to the accurate determination of the contact point and the influence of the substrate underlying thinly spread cells on the measurement of their elastic properties by AFM. The suggested method exploits the main advantages of the AFM technique: the locality of the measurements and the small perturbation imposed on the sample during a measurement.

Materials and methods

Sample preparation

Fresh human RBCs were obtained immediately before the experiment from a healthy volunteer. A small quantity of blood (<100 μL) was washed twice in a PBS solution (137 mM NaCl, 2.7 mM KCl, 10 mM glucose, 1.47 mM KH_2PO_4, 8.1 mM Na_2HPO_4, pH 7.4) and was finally suspended in a PBSA solution (PBS solution containing 0.9 mM $CaCl_2$, 0.49 mM $MgCl_2$, 1 mg/mL bovine serum albumin, pH 7.4). A few drops of the cell suspension, forming a hematocrit of ~0.03%, were spread onto glass coverslips pretreated with a low concentration (~0.06 mg/mL) of poly-L-lysine (MW 32.6 kDa) solution and incubated for 30 min at 37 °C. It enabled the erythrocytes to firmly adhere to the glass substratum, without inducing change in the cell's shape (Tuvia et al. 1997). Unattached cells were removed by gently rinsing the coverglass with PBSA solution.

AFM set-up

Force-distance measurements were recorded using a BioScope atomic force microscope (Digital Instruments, Santa Barbara, Calif.) equipped with a 100-μm XY- and a 7-μm Z-scanner. The AFM was placed on an inverted Zeiss Axiovert 135 microscope. The studies were performed employing silicon nitride cantilevers (Microlevers, Park Scientific Instruments, Sunnyvale), possessing a spring constant of ~0.03 N/m. This choice of a spring constant, which should be smaller than the bending modulus of the cell membrane, is essential for reliable measurements. In order to compare values of the same dimensions, one should choose the two-dimensional equivalent of the Young's modulus corresponding to the bending modulus of the membrane. The acceptable value for the two-dimensional equivalent of the Young's modulus for the RBC membrane is ~450 mN/m (Waugh and Evans 1979), while the spring constant of the AFM cantilever used by us was 30 mN/m. Thus, employing a spring constant of the AFM cantilever, which is 15-fold smaller than the corresponding elastic constant of the cell membrane, enables an accurate measurement of the elastic modulus of the membrane. All force values reported were calculated by using the nominal values of the spring constant. All measurements were carried out in a PBSA solution.

Force measurements

Preceding force-distance measurements on red blood cells, a force plot was performed on a glass substrate in order to avoid artifacts associated with the contamination of the tip's surface. This step was followed by optical-based positioning (brightfield microscopy, ×400) of the tip over the center of the RBC. The force-distance curves were carried out at several scan rates (0.8, 1, 1.5 and 2 Hz) at room temperature. The force was calculated as the product of the cantilever's deflection and its spring constant. Each scanning cycle contained 1024 data points, so that the approach and withdrawal curves consisted of 512 data points each. Each measurement was carried out on a different cell, so the number of experiments for given conditions correspond to the number of tested cells. This was done in order to avoid the problem of the influence of multiple measurements on a single cell and to account for the physiological variability of the cells.

AFM pulling technique

The silicon nitride tips we employed were coated by a cationic polymer following their immersion in an aqueous solution of 1 mg/mL poly-L-lysine for 18 h. Before an experiment the tips were thoroughly rinsed by distilled water. Lowering the tip onto the cell and performing the approach part of the force-distance measurement attained a strong attachment between the tip and the cell membrane. Ensuring a strong attachment of the tip to the membrane enabled the calculation of the elastic property of the cell membrane-skeleton complex from the retraction part (marked by the solid arrow in Fig. 1) of the force-distance measurements. For the sake of briefness, we refer to the membrane-skeleton complex as the cell membrane.

Appropriate force-distance curves were selected based on the criteria discussed in the Results and discussion section. In the selected force-distance curves one can observe the existence of two important points in the withdrawal part. The first point is associated with the exit of the tip from the non-deformed membrane level. The indentation of the cell membrane by the tip produces a concave deformation in the membrane's surface. This indentation diminishes when the tip starts to retract. The point where the tip reaches the level of the resting non-deformed membrane can be defined as an "exit point". The second point in the withdrawal region is the point where a sudden force jump occurs. This point, which can be attributed to the major detachment of the tip from the cell membrane, is defined as "detachment point". The region between these two points can be labeled as the interval corresponding to cell membrane bending (marked by the A–B region between the dotted and solid arrows in Fig. 1).

Theoretical model and data processing

We chose the model of axisymmetric bending of a thick annular plate (Karunasena et al. 1997 and references therein) in order to

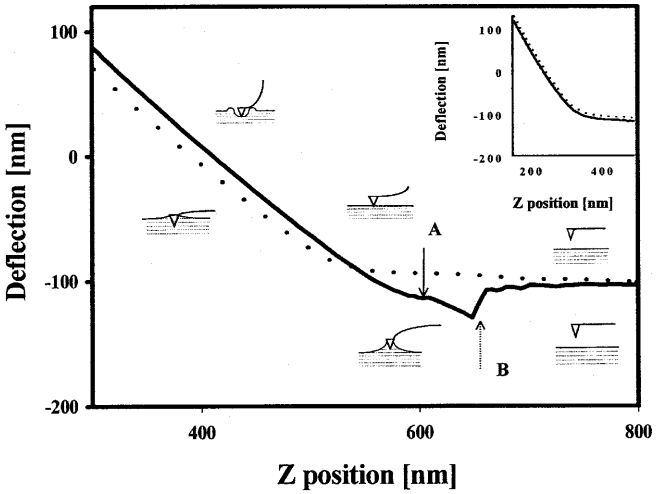

Fig. 1 Scheme of the AFM pulling method. Approach (*dotted line*): the tip is lowered onto the cell surface and starts to deform the cell membrane. Retraction (*solid line*): the tip is withdrawn and starts to pull the cell membrane-skeleton complex until, after further bending, the final detachment occurs in the point marked by the *dotted arrow*. Afterwards, the tip continues its free motion. The *solid arrow* indicates the region where the bud produced by tip indentation disappears owing to the tip withdrawal. This corresponds to the change in the slope of the force-distance dependence. The sketches of the tip's position in the approach are given above the dotted and solid lines, whereas sketches of the tip's position in the withdrawal part are given below the dotted and solid lines. *Insert*: typical pattern of a force-distance plot measured by a non-coated tip. Scan rate was 1 Hz. The zero level for the force is arbitrary, corresponding to the chosen set-point

describe the bending of the cell membrane caused by displacing (pulling) an AFM tip which is attached to the membrane. The model of a circular plate was chosen owing to the fact that part of the membrane which is directly attached to the tip does not deform during the withdrawal of the tip, whereas the membrane located outside the attachment region undergoes deformation. Thus, the traction force acting on the tip can be envisioned as applied to the inner perimeter of a circular plate. When the tip attaches to the membrane, the inner radius will be equal to the linear size of the area of adhesion (''radius of adhesion''). It should be pointed out that this value could be different from the tip radius. Nevertheless, one can prove that the ''radius of adhesion'' is not bigger than the tip radius (see Results and discussion). Therefore in our calculations the inner radius R was equal to the tip radius of 30 nm, providing estimation for the top boundary of the bending modulus. The outer radius r_0 can be estimated from the linear size of the erythrocyte's membrane patches (see Takeuchi et al. 1998 and references therein). The corresponding linear size of the confinement domain in the experiments of band 3 movement tracking (see Tomishige et al. 1998 and references therein) approximately equals 90 nm. Thus the ratio between the outer radius and the inner one can be approximated as 1:3. While the variability of these values is evident, it does not play a significant role owing to the weak dependence of the normalized deflection at the free edge on the ratio between the thickness and the inner radius. Indeed, a 150-fold variation of this ratio yields less than a 3% variation of the normalized deflection at the free edge (see fig. 4 in Karunasena et al. 1997). Furthermore, the thickness of the RBC lipid membrane is about 5 nm and the thickness of glycocalyx-membrane-skeleton complex can be as large as 20 nm. Since in our experiments we restricted the maximal deflection of the membrane by the small value of the standard deviation of the natural fluctuations of the RBC membrane (see selection criteria in Results and discussion), one can expect that the skeleton will not strongly participate in the pulling process. Thus, one can choose the thickness of the plate as equal to 5 nm. Furthermore, the ratio of the membrane thickness to the radius of the inner edge will be approximately equal to 0.16; that again should not influence the accuracy of further calculations owing to the weak dependence of the normalized deflection on this ratio, mentioned above. Nevertheless, since this value is still relatively large, it prohibits the use of a thin plate approximation. Thus, the model should account for the Reissner-Mindlin plate theory (see Karunasena et al. 1997 and references therein). For these conditions, Karunasena et al. present an exact solution in the form:

$$zK_c/PR^3 = 10^{-4}(b_1 + b_2r^2 + b_3 \ln r + b_4r^2 \ln r) \quad (1)$$

where z is displacement, K_c is the bending modulus of the plate, P is the concentric ring load per unit length for the inner plate perimeter, R is the plate inner radius, r is the radial coordinate for which displacement is traced (Fig. 2) and coefficients b_1–b_4 are tabulated in the referenced study for the case where $r_0/R = 3$ (see example 4 and table 4 in Karunasena et al. 1997).

Equation (1) states the existence of a linear relationship between the applied force ($F = P2\pi R$) and the displacement produced, z. The coefficient of proportionality C includes the bending modulus of the plate:

$$C = 10^4 \times 2\pi K_c/R^2(b_1 + b_2r^2 + b_3 \ln r + b_4r^2 \ln r) \quad (2)$$

Therefore, a value of the bending modulus can be estimated from the slope of the force-distance curve in the region corresponding to the bending of the membrane at a constant tip-membrane attachment strength (which enables us to avoid considering additional displacement-dependent forces). The slope can be derived from fitting of the theoretical linear relationship to that part of the experimental curve from the detachment point to an arbitrary point inside the interval corresponding to cell membrane bending. A typical example of fitting is presented in Fig. 3. The actual displacement of the membrane was calculated by subtracting the cantilever deflection from the AFM probe position. All procedures, including opening data files, fitting and recalculation of the bending modulus, were automated by software based on Matlab 5.2, enabling fast processing of hundreds of experimental force-distance curves.

Results and discussion

The bending modulus of the cell membrane was calculated, based on the analysis of the withdrawal region of force-distance curves. A typical pattern of a force-

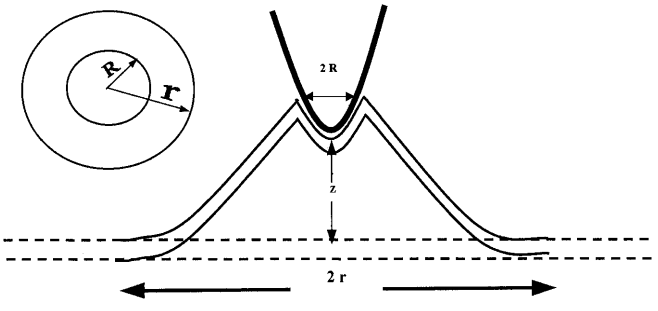

Fig. 2 Theoretical model of axisymmetric bending of a thick annular plate. In the presented scheme, R is the inner radius of the plate that corresponds to the radius of the AFM tip. Part of the membrane attached to the tip does not undergo deformation. The linear size of membrane patch corresponds to the outer radius of the plate r_0. Displacement of any point of the plate can be calculated by following Eq. (1) (see Materials and methods)

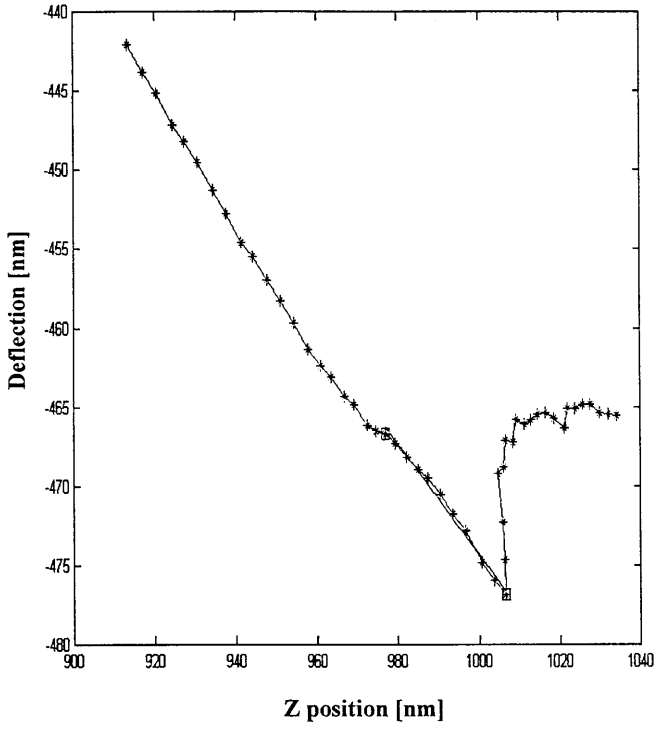

Fig. 3 Fitting procedure for calculation of the bending modulus. An example of the fitting procedure for the linear section of the withdrawal part of a force-distance curve. The theoretical expression of the relationship between membrane displacement and force applied by the AFM probe (*solid line*), which includes the bending modulus as a free parameter, is fitted to the experimental data (*asterisks*)

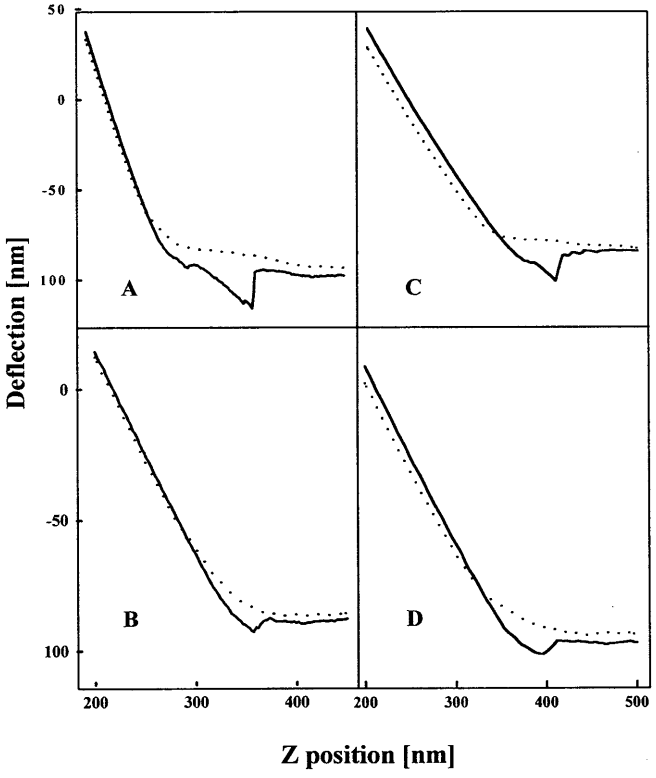

Fig. 4A–D Typical patterns of force-distance curves measured on human erythrocytes. **A** Several step detachment: the tip detaches from the cell membrane by several jumps. **B** Continuous detachment: the tip gradually detaches from the cell membrane; the contact area between the tip and the cell decreases continuously, exerting a distance-dependent friction force between the membrane and tip (see text for further discussion). **C** Single-step detachment: the tip jumps out of contact suddenly after the end of the bending region. **D** Undetermined detachment: the disruption of the tip from the cell membrane is not well determined; therefore analysis is not possible. Scan rate was 1 Hz in each case. The zero level for the force is arbitrary, corresponding to the chosen set-point

distance curve used by us for analysis is presented in Fig. 1. The ability to obtain the appropriate shape of the withdrawal curve in Fig. 1 is based on employing a poly-L-lysine coated tip, which increases the attachment of the tip to the cell membrane. The use of a non-coated tip yields a different pattern for the retraction curve (Fig. 1, insert).

The withdrawal region shown in Fig. 1 is composed of several sections. The first section of the withdrawal region reflects the initial regression of the tip from the stage of the concave deformation of the cell membrane produced by the preceding indentation step. This consequently decreases the deformation of the cell membrane, produced by tip-induced indentation, until attaining a minimal deformation of the membrane. Further withdrawing of the tip generates bending of the cell's membrane. An additional lift of the tip leads to its detachment from the membrane, creating a typical force jump in the force-distance curve, and is followed by further movement of the free tip. However, the shape of the section of interest in the withdrawal region shown in Fig. 1, where the detachment of the tip from membrane takes place, is only one of various possible patterns obtained (Fig. 4).

Not all the experimentally obtained withdrawal curves are suitable for analyzing the bending modulus of the cell membrane, since they may reflect different mechanisms of detachment which result from the interplay of various types of forces. First, there is the force applied by the AFM tip. Second, there is the adhesion force which ensures the transfer of the tip's motion to the cell membrane, i.e. the force which acts between the membrane and the tip. A third type of force is related to the viscoelastic nature of the cell membrane-skeleton complex. A fourth type of force could be significant in the case when the membrane gradually slips off the surface of the withdrawing tip. Thus, for example, Fig. 4A reflects a multi-step detachment, where the tip partially detaches from the cell membrane by several jumps, with partial bending of the membrane. Another type of detachment is of a continuous nature (Fig. 4B), where the tip gradually detaches from the cell membrane, without significant bending of the membrane. In this case the friction force, induced by adhesion interaction between the tip and the cell membrane, will be a significant component in the force balance. Hence, the linear dependence, expected from the theoretical model,

should be disturbed, yielding the shape presented in Fig. 4B. In the absence of elastic forces, the highest absolute value of the force and force jump should be observed at the initial part of the retraction from the "exit point", with a further gradual decrease (see, for example, typical bond breakage curves in Evans and Ritchie 1997). This reflects the existence of the largest number of bonds (largest adhesion force) at the initial stage, followed by a gradual decrease in the number of bonds and the consequent measured force. For example, when the tip is continuously withdrawn and the strength of a single bond is weak, the tip's motion is accompanied by a progressive decrease of the tip area attached to the cell membrane. Thus, further increase of the applied force will lead to gradual detachment of the membrane from the tip. The existence of an additional force (for example, owing to the weak elastic resistance of the membrane) shifts the peak, yielding a V-shaped curve (Evans and Ritchie 1997). Moreover, the friction force between the tip and the membrane can produce a non-linearity on both sides of a V-shaped curve. Another type of force-distance curve is presented in Fig. 4D, where one can see that the rupture event is not well defined, i.e. there is no clear separation between the bending and detachment sections. In this case the analysis is not reliable owing to the uncertainty of the detachment point. In order to establish an approach for examining the elastic behavior of the membrane-skeleton complex solely, devoid of additional contributing uncertainties, we restricted our analysis only to those curves that show a single sudden rupture between the tip and the membrane (Fig. 4C).

In order to be able to choose the withdrawal curves appropriate for analysis, we suggest the following criteria for their selection:

1. The value of the jump at a single detachment point should be at least three-fold higher than the noise level at the out-of-contact region. This has been chosen in order to clearly differentiate between the investigated region of the elastic deformation of the membrane-skeleton and the background noise level.
2. The jumps in the slope of the withdrawal region prior to the final detachment should be comparable with the noise in the out-of-contact region.
3. The existence of a linear region between the "exit point" and the "point of detachment".
4. Since the cell membrane of erythrocytes undergoes spontaneous mechanical fluctuations, possessing a standard deviation of ~30 nm (Strey et al. 1995), the bending of the membrane should not exceed this value. This constraint was set in order to avoid the problems associated with non-local deformations extending over a large area of the cell surface.

The application of the suggested criteria is expected to yield withdrawal curves that correspond to continuous bending of the membrane, followed by a single step of detachment from the tip. These curves are devoid of simultaneous partial bending and detachment, noise blurring and non-local deformations.

A significant feature of the withdrawal part in the measured force-distance curves is the region where the nonlinear dependence of force displacement is transformed into a linear one (see the point marked by the solid arrow in Fig. 1). This region can be attributed to the stage where the tip reaches the level of the non-deformed membrane and where further elevation from this level during the withdrawal stage leads to the initiation of membrane bending. When cell deformation produced in the indentation step occurs, the elastic forces tend to convert the locally deformed membrane into a non-deformed one and the direction of the resultant force coincides with the direction of lifting of the AFM probe. In contrast to this, when the AFM probe is lifted above the level of the non-deformed membrane, producing an increase in the outside bump, the elastic forces start to act in a direction opposite to the tip's motion. This yields a sudden change in the local slope of the withdrawal part of force-distance curves that can be attributed to the tip "exit to exterior". Moreover, it can be pointed out that a further withdrawal of the tip causes a linear dependence of the force on the z-distance from the "exit point" (of the tip from the level of the non-deformed membrane) up to the "detachment point" (see Fig. 1). Thus, the bending of the cell membrane by small local pulling occurs at the interval of the withdrawal part of the force-distance curve, which can be uniquely defined by two points: from the "exit point" to the "detachment point". The natural characteristic of this interval is the corresponding distance which can be interpreted as the maximal displacement of the cell membrane produced by the tip withdrawal from the "exit point" to the "detachment point". It is evident that this value is distributed over a certain range of distances (Fig. 5) owing to the variability of both tip coating conditions and cell surface heterogeneity. We obtained a mean value of maximal displacement of ~30 nm. This value is too large to be attributed to bond breakage, providing evidence for cell membrane bending. Since the number of force-distance curves matching the mentioned criteria was about 80 from the typical total number of processed force-distance curves of about 120 (~66%), we claim that this pattern is predominantly observed in our experiments.

Additional support for membrane bending emerges from the observed dependence of the calculated bending modulus on the scan rate (Fig. 6). This dependence was obtained by performing force-distance measurements at various scan rates. Proceeding with calculations of the bending modulus of the membrane-skeleton complex for each scan rate, one obtains the dependence of the apparent elastic constant on the scan rate. It can be seen that the value of the bending modulus drops with a decrease of the scan rate. Saturation occurs at a scanning frequency of ~1 Hz that corresponds to ~1 ms time interval between two consequent positions of the tip. One should note that there is no statistical difference

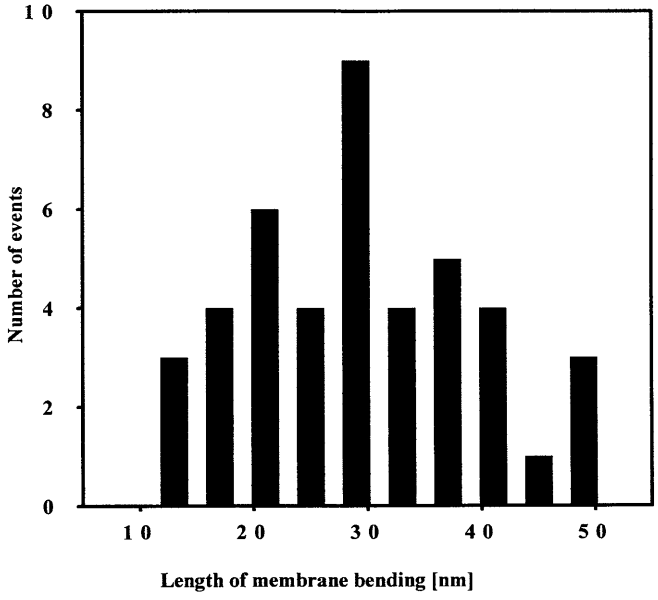

Fig. 5 Histogram of the pulling lengths. Distribution of the pulling lengths in force-distance curves possessing a single-step detachment. The "exit point" is attributed to the exit of the tip from a cell interior. The "detachment point" is defined by the force jump in the withdrawal curve. The length of membrane bending (pulling length) corresponds to the section between the "exit point" and the "detachment point"

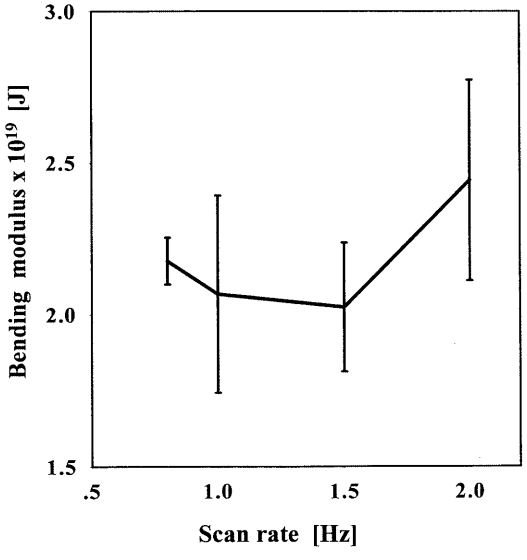

Fig. 6 Dependence of the calculated bending modulus on the scan rate. The difference between bending modulus values for scan rates between 0.8 Hz and 1.5 Hz is not statistically significant. In contrast to this, the difference between the bending modulus value for a scan rate of 2 Hz is statistically different ($P < 0.05$) from the bending modulus values for all other scan rates

between the values of the bending modulus measured at the interval of 0.8–1.5 Hz. However, there was a statistically significant difference ($P < 0.05$) between the bending modulus calculated for 2 Hz and the values obtained for the lower frequencies. If the retraction of the tip would involve only bond-breakage processes, then the corresponding relaxation time should be of the order of ~1 ns (Evans and Ritchie 1997). However, since we obtained an apparent relaxation time of ~1 ms, it cannot be attributed to bond breakage but rather to membrane bending.

The measured dependence of the calculated bending modulus on the scan rate can also assist in avoiding the problem of non-relaxed stress. To clarify this, one can estimate the relaxation time of the long-wavelength fluctuation mode with an amplitude corresponding to the mentioned values of membrane bending introduced by the tip's withdrawal (the value of the step in the z-direction is ~2 nm). The corresponding mode number can be estimated from the well-known expression for the mean squared amplitude of an arbitrary mode (Schneider et al. 1984; Milner and Safran 1987). For the above-mentioned value of 2 nm the mode number is 14–15. The value of the corresponding relaxation time can be calculated by another known expression from fluctuation mode analysis (Schneider et al. 1984; Milner and Safran 1987). This value is about 1 ms. Thus, the characteristic time constant for the relaxation of bending deformations induced by the AFM tip is of the order of 1 ms. Hence, the measured forces will include a partially non-relaxed stress if the characteristic time scale (sampling time) is less than 1 ms (corresponding to scan rates higher than 1–1.5 Hz). Therefore, caution should be taken in measuring elastic constants of composite systems, such as the RBC, and one should try to reduce the additional elastic contributions (stresses) as much as possible. As mentioned, the calculated value of the bending modulus undergoes saturation at the lowest scan rates. The existence of a saturation value suggests that the contribution of the non-relaxed stress to the elastic response be minimized at lower scan rates. The calculated bending modulus for the scan rate of 1 Hz yields a value of $(2.07 \pm 0.32) \times 10^{-19}$ J. This value is in agreement with the value of the bending modulus previously obtained (Evans 1983; Strey et al. 1995).

One should point out that the suggested approach implicitly resolves certain problems associated with participation of different forces in the process of membrane pulling. The experimental data, which are used for the calculation of the bending modulus, is a slope of the linear region in the withdrawal part of the force-distance curve. This slope is the ratio of the difference between forces at the end and at the beginning of the linear region (or between any two values of pulling force inside this region) to the corresponding difference of the membrane deflection values. Such differentiation removes the need for further consideration of all participating forces, which are constant during the short linear interval of pulling, including non-relaxed stress and a strong component of elastic forces produced by sharp bending at the attachment of the membrane to the AFM tip. The last force component should be constant over intervals of ~30 nm deflection (pulling length) and ~30 ms time interval since adhesion conditions and

sharp bending strongly restrict the mobility of molecules of the membrane near the tip. In contrast to this, the relatively free moving molecules outside the region of adhesion will mainly contribute to the elastic response of the membrane to the pulling process.

Our suggested approach, based on atomic force pulling, also possesses certain limitations. To date, the presented method does not allow separating the contributions of the lipid membrane and the underlying skeleton. Indeed, when the AFM tip that is adhered to the membrane starts to pull it, the produced deformation consists not only of the bending deformation of the lipid bilayer, but also of bending and shear deformations of the skeleton. Moreover, the skeleton can also possess strain deformations, which can contribute to the total elastic response. The possible solution of this problem could be based on the difference between relaxation times of the lipid membrane and the skeleton. Another limitation is related to the uncertainty in the determination of the area of membrane adhesion to the tip. While the possibility of measuring this value in our case is very questionable, if at all, one can examine certain consequences from the assumption that fast adhesion occurs mostly at the end of the tip where the curvature of the side walls changes to the curvature of the end. To analyze these consequences one should take into account the existence of strong repulsion forces (so-called Helfrich's forces) between any flexible membrane and a solid body. This interaction builds a barrier that should be overcome in order to bring the membrane and tip into adhesive contact. Applying an external force can carry this out. Indeed, a relatively large external force is applied to the tip during the approach stage. This force, acting almost perpendicularly to the tip surface at its end, ensures fast adhesive contact of the tip end. In contrast to this, a component normal to the side walls of the tip is much smaller owing to the sharpness of the AFM tips. Thus certain additional time will be necessary to establish this contact over the side walls also. Moreover, this time should be independent of the depth of the tip's invasion into the cell if the side wall geometry of the tip does not change much. These assumptions were verified by measurements of pulling length dependence on the time of contact and depth of tip invasion. The measurements under the various times of contact were carried out by the ''ramp delay'' function of the software (Digital Instruments). Since a larger area of adhesion contact provides the possibility to pull the membrane for a longer distance, we choose the pulling length as the parameter characterizing this area. The results are summarized in Table 1. The pulling length does not depend on the depth of tip invasion but depends essentially on the time of contact, as expected from the assumption that fast membrane adhesion occurs mostly at the end of the tip. Furthermore, analysis of the variation coefficient of the ''radius of adhesion'' was carried out in order to estimate the influence of the accuracy of the determination of this parameter on the final results. The estimation was based on the known relationship between the ''radius of adhesion'' and the pull-off critical force (e.g. see eq. 4 in Skulason and Frisbie 2000). We gained a set of force jumps during the breakage of the adhesion contacts from our previously used force-distance curves and calculated the variation coefficient for this set. This coefficient was found to be equal to 0.12. Since the variation coefficient of the ''radius of adhesion'' is a third of the variation coefficient of the pull-off force, it has a value of 0.04. Therefore, the influence of the variation of the ''radius of adhesion'' on the value of the bending modulus is weak.

Table 1 Dependence of the pulling length on the delay and penetration depth. The penetration depth is defined as the maximal indentation or depth of invasion of the membrane into the intracellular matrix produced by the tip at the end of the approach stage. The delay is defined as the time interval when the tip is at the maximal indentation. All pairs of measurements presented in this table were subjected to statistical tests in order to determine whether there is a statistical difference between them. There is no statistical difference (at a level of confidence of 0.95) between measurements corresponding to the different penetration depths. However, there is a statistical difference between measurements corresponding to different delays

Depth (nm)	Delay (s)		
	1	10	20
50	17.5 ± 6	28 ± 10.5	49.2 ± 9.7
80	16.2 ± 3.6	32.6 ± 12.9	51.3 ± 12
120	13.8 ± 2.9	28 ± 7.6	61.4 ± 18

The suggested method resolves some problems related to the measurement of the elastic properties of soft biological materials. Employing the AFM-pulling technique is more reliable in the case of soft and thin structures (e.g. flat cells) on hard substrates, where the supported material can induce an additional error in the definition of the point of contact. Another significant advantage of the suggested method is the small perturbation induced during the measurement. One can point out that we used small perturbations ($\sim$30 nm), but not tethering, which enables us to remain in the range of linear and local deformations. In addition, the problem of the stress induced by the tip motion during the measurements can be corrected (at least partially) in the frame of the suggested method. Thus, the proposed method can be useful for studying the local mechanical properties of living cells.

Acknowledgements This research was supported by the Israel Science Foundation (No. 9002/98-3 to E.B. and R.K.). This work was carried out in partial fulfillment of a PhD requirement of L. Scheffer.

References

A-Hassan E, Heinz WF, Antonik MD, D'Costa NP, Nageswaran S, Schoenenberger C-A, Hoh JH (1998) Relative microelastic mapping of living cells by atomic force microscopy. Biophys J 74:1564–1578

Allen S, Chen XY, Davies J, Davies MC, Dawkes AC, Edwards JC, Roberts CJ, Sefton J, Tendler SJB, Williams PM (1997)

Detection of antigen-antibody binding events with the atomic force microscope. Biochemistry 36:7457–7463
Bezanilla M, Drake B, Nudler E, Kashlev M, Hansma PK, Hansma HG (1994). Motion and enzymatic degradation of DNA in the atomic force microscope. Biophys J 67:1–6
Binnig G, Quate CF, Gerber C (1986) Atomic force microscope. Phys Rev Lett 56:930–933
Brochard F, Lennon JF (1975) Frequency spectrum of the flicker phenomenon in erythrocytes. J Phys (Paris) 36:1035–1047
Evans EA (1983) Bending elastic modulus of red blood cell membrane derived from buckling instability in micropipet aspiration tests. Biophys J 43:27–30
Evans E, Ritchie K (1997) Dynamic strength of molecular adhesion bonds. Biophys J 72:1541–1555
Evans EA, Waugh R, Melnik L (1976) Elastic area compressibility modulus of red cell membrane. Biophys J 16:585–595
Florin EL, Moy VT, Gaub HE (1994) Adhesion forces between individual ligand-receptor pairs. Science 264:415–417
Groner W, Mohandas N, Bessis M (1980) New optical technique for measuring erythrocyte deformability with the ektacytometer. Clin Chem 26:1435–1442
Haydon PG, Lartius R, Parpura V, Marchese-Ragona SP (1996) Membrane deformation of living glial cells using atomic force microscopy. J Microsc 182:114–120
Hoh JH, Schoenenberger C-A (1994) Surface morphology and mechanical properties of MDCK monolayers by atomic force microscopy. J Cell Sci 107:1105–1114
Karunasena W, Wang CM, Kitiporchnai S, Xiang Y (1997) Exact solutions for axisymmetric bending of continuous annular plates. Comput Struct 63:455–464
Koutsoris D, Guillet R, Lelievre JC, Guillemin MT, Bertholm P, Beuzard Y, Boynard M (1988) Determination of erythrocyte transit times through micropores. I. Basic operational principles. Biorheology 25:763–772
Laney DE, Garcia RA, Parsons SM, Hansma HG (1997) Changes in the elastic properties of cholinergic synaptic vesicles as measured by atomic force microscopy. Biophys J 72:806–813
Milner ST, Safran SA (1987) Dynamical fluctuations of droplet microemulsions and vesicles. Phys Rev A 36:4371–4379
Radmacher M, Fritz M, Kacher CM, Cleveland JP, Hansma PK (1996) Measuring the viscoelastic properties of human platelets with the atomic force microscope. Biophys J 70:556–567
Schmid-Schonbein H, Gosen J, von Heinich L, Klose HJ, Volger E (1973) A counter-rotating ''rheoscope chamber'' for the study of the microrheology of blood cell aggregation by microscopic observation and microphotometry. Microvasc Res 6:366–376
Schneider MB, Jenkins JT, Webb WW (1984) Thermal fluctuations of large quasi-spherical bimolecular phospho-lipid vesicles. J Phys (Paris) 45:1457–1472
Shroff SG, Saner DR, Lal R (1995) Dynamic micromechanical properties of cultured rat atrial myocytes measured by atomic force microscopy. Am J Physiol 269:C286–C289
Skulason H, Frisbie CD (2000) Rupture of hydrophobic microcontacts in water: correlation of pull-off force with AFM tip radius. Langmuir 16:6294–6297
Strey H, Peterson M, Sackmann E (1995) Measurement of erythrocyte membrane elasticity by flicker eigenmode decomposition. Biophys J 69:478–488
Takeuchi M, Miyamoto H, Sako Y, Komizu H, Kusumi A (1998) Structure of the erythrocyte membrane skeleton as observed by atomic force microscopy. Biophys J 74:2171–2183
Thomson NH, Fritz M, Radmacher M, Cleveland JP, Schmidt CF, Hansma PK (1996) Protein tracking and detection of protein motion using atomic force microscopy. Biophys J 70: 2421–2431
Tomishige M, Sako Y, Kusumi A (1998) Regulation mechanism of the lateral diffusion of band 3 in erythrocyte membranes by the membrane skeleton. J Cell Biol 142:989–1000
Tuvia S, Almagor A, Bitler A, Levin S, Korenstein R, Yedgar S (1997) Cell membrane fluctuations are regulated by medium macroviscosity: evidence for a metabolic driving force. Proc Natl Acad Sci USA 94:5045–5049
Waugh RE, Evans EA (1979) Thermoelasticity of red blood cell membrane. Biophys J 26:115
Zilker A, Ziegler M, Sackmann E (1992) Spectral analysis of erythrocyte flickering in the 0.3–4 μm^{-1} regime by microinterferometry combined with fast image processing. Phys Rev A 46:7998–8001